

Physical Limit of Stability in Supercooled Liquids¹

S. B. Kiselev²

The kinetic spinodal (KS) in supercooled liquids, similar to the KS in superheated and stretched liquids, has been introduced as a locus where the mean time of formation of a critical nucleus becomes shorter than a relaxation time to local equilibrium. If the surface tension of the solid–liquid interface is known, the kinetic spinodal is completely determined by the equation of state of the supercooled liquid. The theory was tested against experimental data for the surface tension and the homogeneous nucleation limit for supercooled water. Reasonably good agreement between theoretical predictions and experimental data was observed. A prediction of the high-temperature limit for glass transitions is also discussed.

KEY WORDS: glass transition; homogeneous nucleation; kinetic spinodal; supercooled water; surface tension.

1. INTRODUCTION

In the usual thermodynamic theory of phase transitions, the spinodal, the locus of states of infinite compressibility, is considered a boundary of the metastable states in fluids [1]. However, physically the metastable state becomes short-lived well before the spinodal is reached [2, 3]. According to the classical theory of homogeneous nucleation, the lifetime of the metastable state is determined by the mean time of formation of a critical nucleus of the stable phase t_M , which depends on both the thermodynamic and the transport properties of the fluid (for a review, see Ref. 4). In this theory, a metastable phase is considered a short-lived, but still thermodynamic, state of a metastable fluid. In the fluctuation theory of relaxation of metastable states developed by Patashinskii and Shumilo [5, 6], the physical

¹ Paper presented at the Fourteenth Symposium of Thermodynamic Properties, June 25–30, 2000, Boulder, Colorado, U.S.A.

² Chemical Engineering Department, Colorado School of Mines, 1500 Illinois Street, Golden, Colorado 80401-1887, U.S.A. E-mail: skiselev@mines.edu

boundary of metastable states was introduced as a locus where the mean time of formation of a critical nucleus of the stable phase, t_M , becomes shorter than a characteristic time governing the decay of fluctuations to local equilibrium, t_R . When $t_M \leq t_R$, the entire concept of a homogeneous state ceases to be valid, and as a result of fluctuations, the initial homogeneous state transforms to a heterogeneous state during the time $t \approx t_R$ [6]. Both times, t_M and t_R , depend on the kinetic properties of the liquid, but the ratio t_M/t_R depends only on the thermodynamic properties. Therefore, the physical boundary of the metastable state, or kinetic spinodal, is completely determined by the equation of state and the surface tension.

In the present work, we continue the study of the kinetic boundary of metastable states in fluids initiated in our previous studies of vapor–liquid equilibrium [7, 8]. Here we extend this approach to solid–liquid equilibrium and consider the kinetic boundary of metastable states in supercooled liquids. The theory was tested against experimental data for supercooled water.

2. THEORETICAL BACKGROUND

The dynamics of a system in the metastable state of the initial phase is connected with the relaxation and fluctuations of the hydrodynamic fields of the order parameter $\varphi(\vec{x}, t)$, energy density $\varepsilon(\vec{x}, t)$, etc. [5, 6]. The slowness of their relaxation allows us to exclude other degrees of freedom that supposedly reach local equilibrium. In liquids, we may consider the dynamics of a single hydrodynamic mode, which is a scalar field of the order parameter only. In this case, the equation of motion of the system is [9]

$$\frac{\partial \varphi}{\partial t} = -\Gamma_c \Delta \left(\frac{\partial H}{\partial \varphi} + f_{st} \right) \quad (1)$$

where Γ_c is the transport coefficient, H is the effective Hamiltonian, and f_{st} is an external random force modeling the thermal fluctuations. The effective Hamiltonian $H\{\varphi\}$ can be expanded in a functional series as in a second-order phase transition. In the vicinity of the stable region, the effective Hamiltonian can be represented in the form [6]

$$H\{\varphi\} = \int d^3r \left(\frac{g}{2} (\nabla \varphi)^2 + \frac{u_2}{2} \varphi^2 + \frac{u_3}{3} \varphi^3 \right) \quad (2)$$

where g , u_2 , and u_3 are positive constants, and u_2 is assumed to be small. The curve $u_2 = 0$ represents a bare or “unrenormalized” spinodal (i.e.,

a spinodal of the system in the absence of fluctuations). The solution of Eqs. (1) and (2), which was obtained by Patashinskii and Shumilo [5, 6], yields a lifetime of the metastable phase, which accounts for fluctuations and is given by the following equation:

$$t_M = t_R \left(\frac{4\pi\gamma}{\lambda_0} \right) \exp(\gamma W_{\min}/k_B T) \quad (3)$$

where $t_R = 16g/(\Gamma_0 u_2^2)$ is a characteristic time governing the relaxation toward local equilibrium, W_{\min} is the nucleation barrier, which is equal to the minimum reversible work required to form a critical size nucleus, the dimensionless parameter $\gamma = (u_2 g)^{3/2}/(k_B T u_3^2)$, and $\lambda_0 \cong 8.25$ is a dimensionless constant. It follows from Eq. (3) that when $\gamma W_{\min} \gg k_B T$ the lifetime of the metastable phase is much longer than the relaxation time t_R . For $\gamma < k_B T/W_{\min}$, the initial homogeneous state that is stable with respect to long-wavelength fluctuations transforms to a heterogeneous state as a result of fluctuations during a time comparable with the time governing the relaxation toward local equilibrium ($t_M \cong t_R$). The curve $\gamma W_{\min} = k_B T$, or, alternatively,

$$u_2 = (u_2)_{KS} = \frac{1}{g} \left[\frac{(k_B T u_3)^2}{W_{\min}} \right]^{2/3} \quad (4)$$

can be regarded as the physical (kinetic) spinodal, which limits the region in the phase diagram [$u_2 > (u_2)_{KS}$] of statistically well-defined and experimentally attainable metastable states. For $0 < u_2 < (u_2)_{KS}$, the lifetime $t_M < t_R$ and the very concept of an equilibrium homogeneous state is no longer applicable, and this spinodal region separates metastable and unstable states in the phase diagram of one-component fluids.

To use the theoretical result contained in Eq. (4) for practical calculations of the kinetic boundary of metastable states, we need to know how the parameters u_2 , u_3 , and g of the effective Hamiltonion in Eq. (2) are related to the thermodynamic parameters of the real physical system. As shown in our previous work [7, 8], the parameters u_2 and u_3 are directly related to the first and second derivatives of the chemical potential, μ , with respect to the density

$$u_2 = \rho^2 \left(\frac{\partial \mu}{\partial \rho} \right)_T = k_B T \rho \bar{\mu}_\rho, \quad u_3 = \frac{1}{2} \rho^3 \left(\frac{\partial^2 \mu}{\partial \rho^2} \right)_T = \frac{1}{2} k_B T \rho \bar{\mu}_{\rho\rho} \quad (5)$$

and for the parameter g a good estimate is

$$g = k_B T (\rho^*)^{1/3} \quad (6)$$

where ρ^* is a characteristic density in the system. In superheated and stretched liquids we used the critical density ρ_c [7, 8] as a characteristic density in Eq. (6), while in supercooled liquids one can set ρ^* equal to the density of the liquid at the triple point, $\rho^* = \rho_{tr}$.

Finally, with the use of Eqs. (5) and (6), Eq. (4) for the kinetic spinodal T_{KS} in supercooled liquids can be written in the form

$$\bar{\mu}_\rho(T_{KS}) = \left[\frac{k_B T \bar{\mu}_{\rho\rho}^2(T_{KS})}{4W_{\min}(T_{KS})} \right]^{2/3} \left(\frac{\rho}{\rho_{tr}} \right)^{1/3} \quad (7)$$

where the nucleation barrier for the spherical crystal nucleus in supercooled liquids is given by [2, 3]

$$W_{\min} = \frac{16\pi T_m^2(P) \sigma_{SL}^3(T) v_s^2(T)}{3 \Delta h^2 \Delta T^2} \quad (8)$$

Here σ_{SL} is the surface tension at the liquid–crystal interface, v_s is the molar volume of the crystal, Δh is the molar enthalpy of fusion, T_m is the melting temperature at a given pressure P , and $\Delta T = T_m - T$ is the degree of supercooling.

3. COMPARISON WITH EXPERIMENTAL DATA

To calculate the kinetic boundary of the metastable state with Eq. (7), one needs to know the equation of state (EOS) (which can be extrapolated into the metastable region) and the surface tension. For vapor–liquid equilibrium the equation of state and the surface tension are usually well known, and the kinetic spinodal in superheated and stretched liquids can be predicted with a high accuracy [7, 8]. In supercooled liquids, the situation is more complicated. The equation of state obtained from the analysis of the experimental data for a stable liquid, as a rule, cannot be extrapolated into the supercooled region, and the solid–liquid surface tension is usually unknown. Unlike the vapor–liquid surface tension, the solid–liquid surface tension cannot be measured directly and it is usually determined from the analysis of experimental data for the nucleation rate in the supercooled liquid [2]. It is clear that the numerical value of the surface tension obtained by this method depends strongly on the theoretical model applied for this analysis. This increases the uncertainties in the prediction of the kinetic boundary of the metastable state in supercooled liquids.

For a comparison of the theory with experimental data, we consider here the thermodynamic properties of supercooled water. For supercooled water, most of the information about the surface tension was obtained at atmospheric pressure; therefore, we first consider here the isothermal

compressibility, K_T , and homogeneous nucleation temperature, T_H , data obtained at $P = 0.1$ MPa by Speedy and Angell [10]. The surface tension σ_{SL} was obtained from a solution of Eq. (7) for the kinetic spinodal where we set $T_{KS} = T_H$, with $T_H = 235.16$ K as obtained by Speedy and Angell [10]. For the representation of the thermodynamic properties of water the IAPWS-95 formulation [11] is recommended as the most accurate. As pointed out in an IAPWS release [11], this formulation behaves reasonably when extrapolated into the metastable region and represents the available experimental data of supercooled water to within the experimental uncertainty. However, it is not clear how this EOS represents the second derivatives of the pressure with respect to density in supercooled water at temperatures close to T_S . Therefore, to avoid a misinterpretation of experimental data, the density of the liquid and the second derivative $\bar{\mu}_{\rho\rho}$ in Eq. (7) were calculated with the IAPWS-95 formulation [11] at the melting temperature T_m . Since at low pressures near the melting curve, ρ and $\bar{\mu}_{\rho\rho}$ are slowly varying quantities, we assume that this is a reasonable approximation. We calculate the first derivative $\bar{\mu}_\rho(T) = K_T^{-1}/\rho RT$ with an empirical expression for the isothermal compressibility,

$$K_T = A_\kappa (T/T_S - 1)^{-\gamma_\kappa} \quad (9)$$

where the parameters $A_\kappa = 296.5 \times 10^{-6}$ MPa, $\gamma_\kappa = 0.349$, and $T_S = 228$ K were obtained by Speedy and Angell [10] from a fit of Eq. (9) to their experimental data in supercooled water at $P = 1$ MPa. The melting temperature T_m was calculated with the international equation developed by Wagner et al. [12], while for the calculation of the ice density, ρ_S , and heat of fusion, Δh , we used the vapor pressure formulation for ice developed by Wexler [13].

The result of our calculations in comparison with the values of surface tension obtained by other authors is shown in Fig. 1. Our value of surface tension lies between the values of $\sigma_{SL} = 0.0287 \text{ J} \cdot \text{m}^{-2}$ and $\sigma_{SL} = 0.0240 \text{ J} \cdot \text{m}^{-2}$ obtained at the same temperature by Butorin and Skripov [14] and by Wood and Walton [15], respectively. The surface tensions reported in Refs. 14 and 15 were obtained from an analysis of the nucleation rate data and, as pointed out by Butorin and Skripov [14], the difference between them is due to an additional temperature-dependent factor, $(T_m/T)^2$, introduced into the equation for the nucleation barrier, Eq. (8), by Wood and Walton [15]. Our value of the surface tension, $\sigma_{SL} = 0.0258 \text{ J} \cdot \text{m}^{-2}$, was obtained from a different theoretical model. Therefore, the difference of about $\pm 8\%$ obtained for σ_{SL} in our case can be considered as reasonably small in view of the uncertainty of nucleation theory. Huang and Bartell [16], for example, obtained the same difference using slightly different

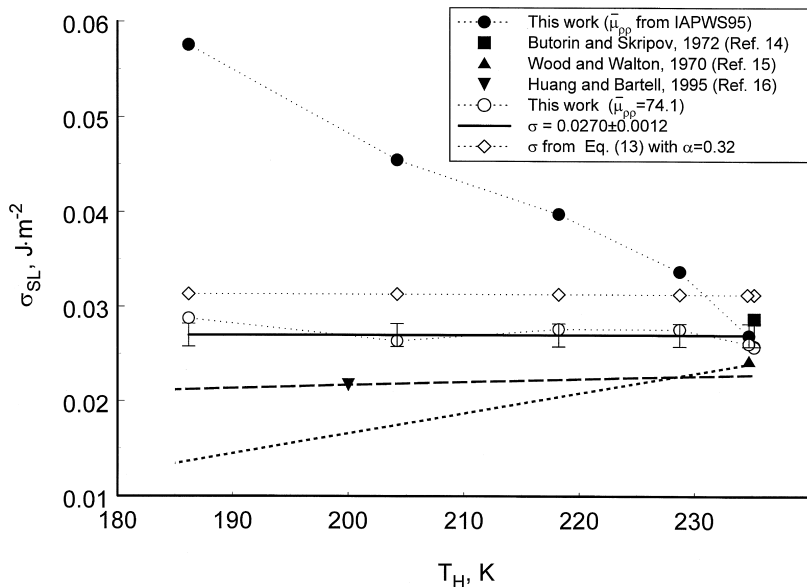


Fig. 1. The ice water surface tension as a function of temperature. The filled circles with the dotted eye-guide lines represent the values calculated with Eq. (7) with $T_{KS} = T_H$ and $\bar{\mu}_{pp}(T_m)$ obtained from the IAPWS-95 formulation [11] at different pressures along the melting curve, the open circles correspond to the values calculated with Eq. (7) with $\bar{\mu}_{pp} = 74.1$, and the open diamonds correspond to the values calculated with Eq. (13) with $\alpha = 0.32$. The filled symbols correspond to experimental data obtained by Butorin and Skripov [14] (squares), by Wood and Walton [15] (up triangles), and by Huang and Bartell [16] (down triangles). The solid line corresponds to the constant value $\sigma_{SL} = 0.027 \text{ J} \cdot \text{m}^{-2}$; the long- and short-dashed lines represent the values calculated with Eq. (25) in Ref. 15 and with Eq. (3) in Ref. 16, respectively.

modifications of kinetic theory for the analysis of their nucleation rate experimental data at $T = 200 \text{ K}$. At lower temperatures this difference can even increase. A power-law interpolation,

$$\sigma(T) = \sigma(T_1)(T/T_1)^{0.3} \quad (10)$$

proposed by Huang and Bartell [16] is also shown in Fig. 1. At $T = 235 \text{ K}$, the power-law interpolation gives $\sigma_{SL} = 0.0228 \text{ J} \cdot \text{m}^{-2}$, which is about 5% lower than the value obtained by Wood and Walton [15]. While at low temperatures, $T < 200 \text{ K}$, the values of surface tension calculated with this interpolation lie about 20–40% higher than those obtained from the simple linear interpolation,

$$\sigma(T) = \sigma(T_1) + (d\sigma/dT)_{T_1} (T - T_1) \quad (11)$$

using $(d\sigma/dT)_{T=-36.55^\circ\text{C}} = 0.211 \times 10^{-2} \text{ J} \cdot \text{m}^{-2}$, obtained by Wood and Walton [15].

To estimate the values of the surface tension at other temperatures, we applied the above procedure to isothermal compressibility and homogeneous nucleation data obtained by Kanno and Angell [17] at higher pressures, up to 190 MPa. The filled circles in Fig. 1 show the values of the surface tension obtained with this method. One can see that despite expectation, the surface tension extracted from our theory in this case increases with a decrease in temperature. Such behavior of the surface tension is specific for the heterogeneous nucleation that can be observed in large volumes [14], rather than for the homogeneous nucleation in small droplets. In Fig. 2, we show the critical radius of the nucleus [2, 3]

$$r_c = \frac{2T_m(P) \sigma_{\text{SL}}(T) v_s(T)}{\Delta h \Delta T} \quad (12)$$

calculated with different models for the surface tension at the homogeneous nucleation temperatures reported by Kanno and Angell [17]. At low temperatures, $T < 200 \text{ K}$, the critical radius of the nucleus calculated with

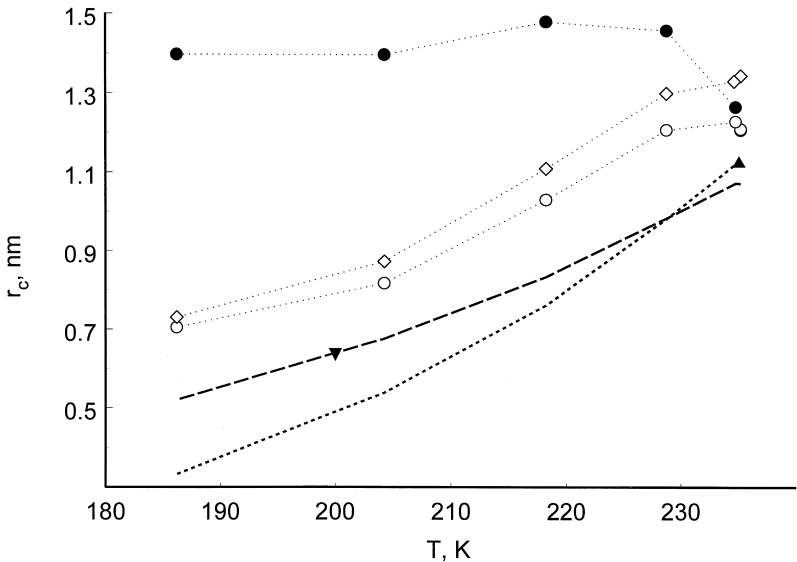


Fig. 2. The critical radius of the nucleus in supercooled water as a function of temperature. The legend is the same as for Fig. 1.

Eqs. (10) and (11), $r_c \simeq 0.3$ to 0.9 nm, becomes comparable with the characteristic size of the network defects in liquid water [18]. In principle, in this case the network defects can play the role of the nucleation centers and can stimulate heterogeneous nucleation even in small droplets. Although there are also some other indications that liquid water can exist down to $T = 150$ K [19], we have no solid evidence that the data reported by Kanno and Angell [17] correspond to heterogeneous nucleation. Therefore, we assume here that this unusual temperature behavior of the surface tension is a result of extrapolation of the quantity $\bar{\mu}_{pp}$ obtained at the melting temperature to the homogeneous nucleation temperature T_H at these pressures. To avoid this “illegal” extrapolation of the quantity $\bar{\mu}_{pp}$ into the metastable region at high pressures, we, in the second step, used, at all pressures, the value $\bar{\mu}_{pp} = 74.1$ obtained at $P = 0.1$ MPa. The results for the surface tension obtained with this constant value of the parameter $\bar{\mu}_{pp}$ are shown in Fig. 1 by open circles. In this case, over the entire temperature range $180 \text{ K} < T < T_m$, the surface tension can be treated as a temperature-independent constant, $\sigma_{SL} = 0.0270 \pm 0.0012 \text{ J} \cdot \text{m}^{-2}$. This value is about 20% larger than the values obtained from the power-law interpolation of Huang and Bartell [16] and about 20% smaller than values calculated from Turnbull’s expression [20]

$$\sigma_{SL} = \alpha \frac{\Delta h}{v_s^{2/3}} \quad (13)$$

with $\alpha = 0.32$, originally recommended for water by Turnbull [20].

In Fig. 3, we show the temperatures at the kinetic spinodal, T_{KS} , calculated from Eq. (7) with the surface tension $\sigma_{SL} = 0.0270 \text{ J} \cdot \text{m}^{-2}$ and with the surface tension calculated with Eq. (13). In both cases, T_{KS} satisfies the obvious condition $T_S < T_{KS} \leq T_H$, or, equivalently, $(u_2)_S < (u_2)_{KS} < (u_2)_H$. Since the kinetic spinodal represents the boundary behind which no equilibrium thermodynamic state can exist, here we consider the lowest temperatures [i.e., T_{KS} calculated with the surface tension as given by Eq. (13)] as a physical boundary of metastable states in supercooled water. The shaded area in Fig. 3 marks the “nonthermodynamic habitat” for liquid water, i.e., the region where no thermodynamic state for liquid water is possible. It is not because in this region the parameter $\bar{\mu}_p < 0$, which violates the thermodynamic condition of mechanical stability. The first derivative $\bar{\mu}_p$, or, equivalently, the parameter u_2 in Eq. (2), can remain small but positive in this region. It is a “nonthermodynamic habitat” because the lifetime of the homogeneous state in this region is smaller than the time to establish local equilibrium. Therefore, any equilibrium homogeneous state for liquid water is not possible in this region.

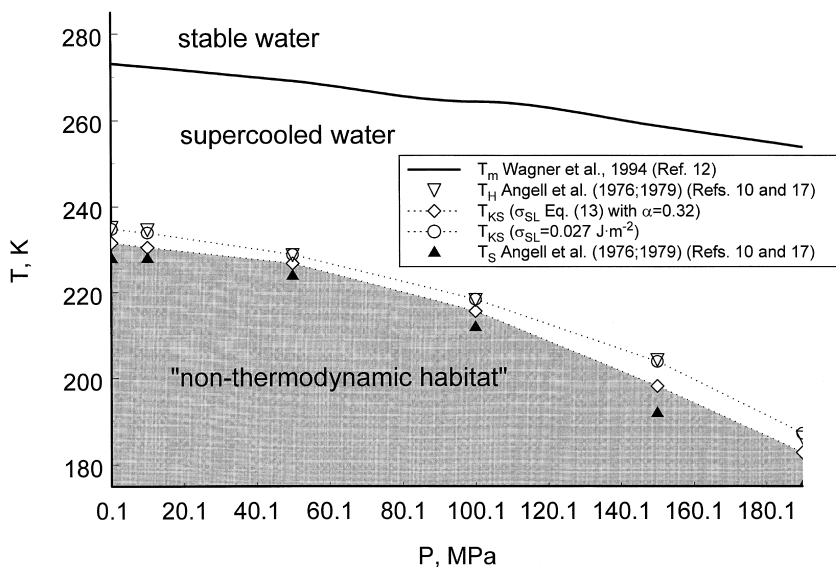


Fig. 3. The phase diagram of supercooled water. The solid line represents the melting curve [12]; the open diamonds and circles with the eye-guide lines correspond to the kinetic spinodal temperatures, T_{KS} , calculated with Eq. (7) with different approximations for the surface tension; and the symbols represent the homogeneous nucleation, T_H (down triangles), and spinodal, T_S (up triangles), temperatures obtained by Angell et al. [10, 17].

4. DISCUSSION

In the present work, we have developed a general approach for predicting the physical boundary of metastable states—the kinetic spinodal in supercooled liquids. This approach requires only the EOS and the solid–liquid surface tension for accurate prediction of the kinetic spinodal in supercooled liquids. The approach can be applied to any supercooled liquid with the scalar order parameter, including liquid metals. Here we applied this method for calculation of the surface tension and the kinetic spinodal in supercooled water. Reasonably good agreement with experimental data was achieved.

Although water is the most common and best-studied liquid, the peculiar behavior of its physical properties in the supercooled regime is still a puzzle for investigators [21], and water remains the most difficult fluid for modeling. Only during the last 4 to 5 years have several models and EOSs been developed to represent the anomalous behavior of liquid water in the supercooled regime [22–29]. These models give different, and even alternative, scenarios of the behavior of supercooled water, and at the

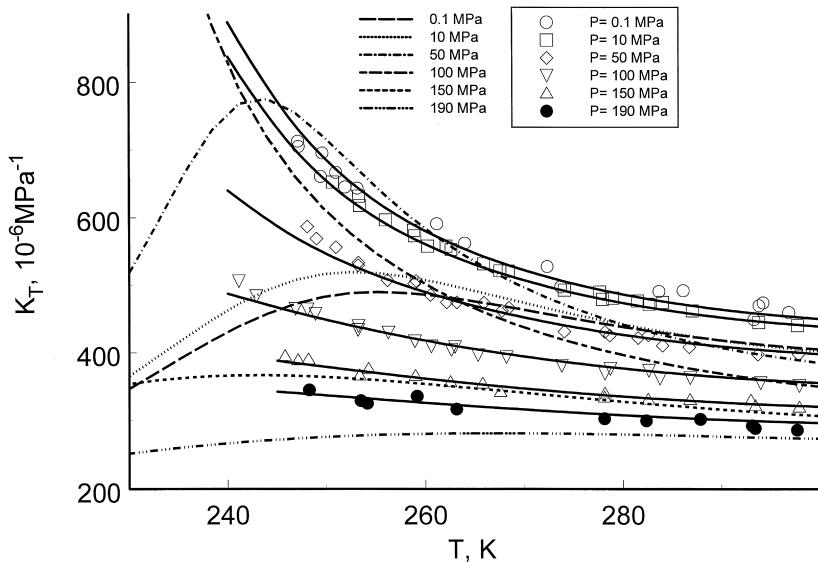


Fig. 4. The isothermal compressibility of water at different pressures in normal and supercooled states as a function of temperature. The symbols represent experimental values obtained by Angell et al. [10, 17], the solid curves represent values calculated with the IAPWS-95 formulation [11], and the dotted-dashed curves correspond to the values calculated with the new analytic equation of state of Jeffery and Austin [29].

present time, it is not clear which of them is correct. Our approach can be used as a test of the thermodynamic consistency of the developed models in the supercooled region, as done in superheated and stretched water [30].

As an example, we applied this method to the new analytical (NA) equation of state for supercooled water developed recently by Jeffery and Austin [29]. This equation predicts the existence of the second critical point (CP_2) related to the low-density water (LDW)/high-density water (HDW) phase equilibrium and qualitatively reproduces the anomalous behavior of the isothermal compressibility in supercooled water. However, the quantitative difference between the experimental and the calculated values of the isothermal compressibility in supercooled water is significant (see Fig. 4). Because of the positions of the CP_2 ($T_{c2} = 228.3$ K, $P_{c2} = 95.3$ MPa, and $\rho_{c2} = 1042$ kg·m⁻³), the maximum compressibility calculated with the NA EOS corresponds to the isobar $P = 100$ MPa, but not to $P = 0.1$ MPa, as observed in the experiment. As a consequence, the kinetic spinodal calculated with this EOS lies above the homogeneous nucleation temperatures, which is physically incorrect. The phase diagram and the kinetic spinodal calculated with this equation are shown in Fig. 5. The

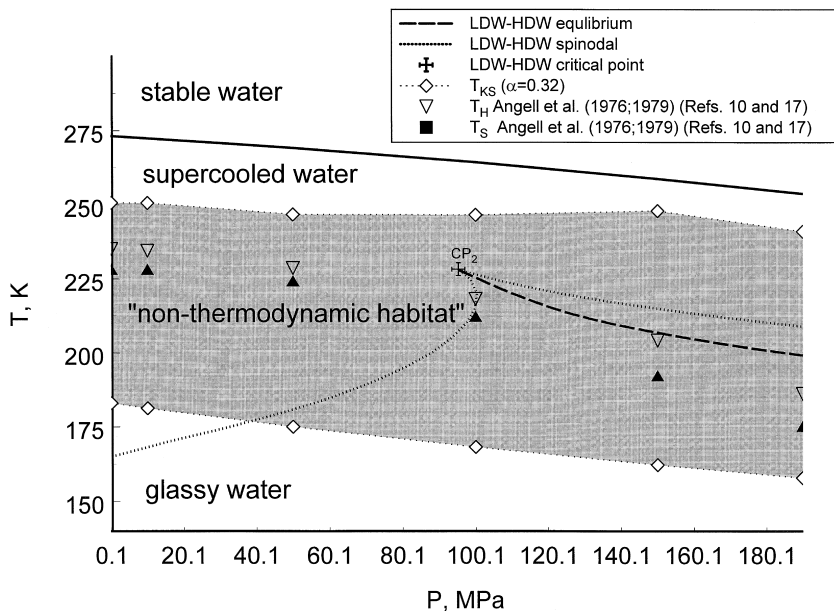


Fig. 5. The phase diagram of supercooled water calculated with the new analytic equation of state of Jeffery and Austin [29]. The cross corresponds to the critical point of LDW–HDW equilibrium (dashed curve); the dotted curves correspond to the LDW–HDW spinodals. Otherwise the legend is the same as for Fig. 2.

principle differences between this diagram and the phase diagram in Fig. 3 are that Eq. (7) now has two roots, T_{KS1} and T_{KS2} , and the “nonthermodynamic habitat” for supercooled liquid water now has the shape of the belt. The second critical point and the LDW–HDW coexistence curve lie inside the nonthermodynamic habitat belt, and therefore, they have no physical meaning. Nevertheless, in principle, the conception of the second, “virtual critical point” can be useful if it yields a good representation of the thermodynamic properties of supercooled water outside the nonthermodynamic habitat belt created by this virtual critical point itself.

A possible physical interpretation of the second kinetic spinodal temperature T_{KS2} is that this temperature corresponds to the upper temperature limit where the glass transition at a given pressure is possible. For example, at $P = 0.1$ MPa, the temperature T_{KS1} calculated with the NA EOS [29] is about 16 K higher than the homogeneous nucleation temperature obtained by Speedy and Angell [10]. After a shift of the second kinetic spinodal temperature T_{KS2} at the same value, one obtains $T_{KS2}^{\text{shift}} = 167$ K, which is a reasonable estimate for the glass transition limit at this pressure. To give a

more accurate prediction of the glass transition limit in supercooled liquids, we need both a better EOS and additional theoretical study of this phenomenon.

ACKNOWLEDGMENTS

The author is indebted to A. H. Harvey for helpful comments and to P. H. Austin for providing his computer program for calculation of the thermodynamic properties of metastable water. This research was supported by the U.S. Department of Energy, Office of Basic Energy Sciences, under Grant DE-FG03-95ER14568.

REFERENCES

1. L. D. Landau and E. M. Lifshitz, *Statistical Physics, Part 1* (Pergamon Press, New York, 1980).
2. V. P. Skripov, *Metastable Liquids* (John Wiley & Sons, New York, 1972).
3. P. G. Debenedetti, *Metastable Liquids: Concepts and Principles* (Princeton University Press, Princeton, NJ, 1996).
4. F. F. Abraham, *Homogeneous Nucleation Theory* (Academic Press, New York, 1974)
5. A. Z. Patashinskii and B. I. Shumilo, *Sov. Phys. JETP* **50**:712 (1979).
6. A. Z. Patashinskii and B. I. Shumilo, *Sov. Phys. Solid State* **22**:655 (1980).
7. S. B. Kiselev, J. M. H. Levelt-Sengers, and Q. Zheng, in *Physical Chemistry of Aqueous System: Meeting the Needs of Industry*, H. J. White, J. V. Sengers, D. B. Neumann, and J. C. Bellows, eds. (Begell House, New York-Wallingford, 1995), p. 378.
8. S. B. Kiselev, *Physica A* **269**:252 (1999).
9. A. Z. Patashinskii and V. L. Pokrovskii, *Fluctuation Theory of Phase Transitions*, 3rd ed. (Pergamon, New York, 1979).
10. R. J. Speedy and C. A. Angell, *J. Chem. Phys.* **65**:851 (1976).
11. *Release of the IAPWS Formulation 1995 for the Thermodynamic Properties of Ordinary Water Substance for General and Scientific Use* (Frederica, Denmark, 1996). Available from the IAPWS Executive Secretary: Dr. R. B. Dooley, Electric Power Research Institute, 3412 Hillview Avenue, Palo Alto, CA 94304, U.S.A.
12. W. Wagner, A. Saul, and A. Pruss, *J. Phys. Chem. Ref. Data* **23**:515 (1993).
13. A. Wexler, *J. Res. Natl. Bur. Stand.* **81A**:5 (1976).
14. G. T. Butorin and V. P. Skripov, *Sov. Phys. Crystallogr.* **17**:322 (1972).
15. G. R. Wood and A. G. Walton, *J. Appl. Phys.* **41**:3027 (1970).
16. J. Huang and L. S. Bartell, *J. Phys. Chem.* **99**:3924 (1995).
17. H. Kanno and C. A. Angell, *J. Chem. Phys.* **70**: 4008 (1979).
18. F. Sciortino, A. Geiger, and H. E. Stanley, *J. Chem. Phys.* **96**:3857 (1992).
19. R. S. Smith and B. D. Kay, *Nature* **398**:788 (1999).
20. D. Turnbull, *J. Appl. Phys.* **21**:1022 (1950).
21. H. E. Stanley, S. V. Buldyrev, M. Canpolat, S. Havlin, and O. Mishima, *Physica D* **133**:453 (1999).
22. S. Sastry, P. G. Debenedetti, F. Sciortino, and H. E Stanley, *Phys. Rev. E* **53**: 6144 (1996).
23. F. Sciortino, P. H. Poole, U. Essmann, and H. E. Stanley, *Phys. Rev. E* **55**:727 (1997).
24. L.P.N. Rebelo, P. G. Debenedetti, and S. Satry, *J. Chem. Phys.* **109**:626 (1998).

25. M.T. Truskett, P. G. Debenedetti, S. Sastry, and S. Torquato, *J. Chem. Phys.* **111**:2647 (1999).
26. H. Tanaka, *J. Chem. Phys.* **105**:5099 (1996).
27. L. S. Bartell, *J. Phys. Chem.* **101**:7573 (1997).
28. E. G. Ponyatovsky, V. V. Sinitsyn, and T. A. Pozdnyakova, *J. Chem. Phys.* **109**:2413 (1998).
29. C. A. Jeffery and P. H. Austin, *J. Chem. Phys.* **110**:484 (1999).
30. S. B. Kiselev, J. M. H. Levelt-Sengers, H. Sato, and Q. Zheng, *Metastable States of Water and Steam. Part III. Physical Limits of the Stability of water. Implications for Formulations*. Report to the IAPWS Meeting, Sept. 30 (1993).